



International journal of basic and applied research

www.pragatipublication.com

ISSN 2249-3352 (P) 2278-0505 (E)

Cosmos Impact Factor-5.86

AN EFFICIENT INDUCTIVE POWER TOPOLOGY FOR ELECTRIC VEHICLE BATTERY CHARGING

M.Nagaraju¹, T.Vardhan², M.Venkata Jaswanth³, P.Sai Meghana⁴, T.Tejaswini⁵,

B.Suresh⁶, J.Srinivasa Rao⁷

^{1,2,3,4,5,6} Under Graduate in Department of EEE

⁷ Assistant Professor in Department of EEE

^{1,2,3,4,5,6,7} QIS College Of Engineering and Technology

ABSTRACT

Over the last ten years, this project's vehicle-to-grid idea has garnered a lot of attention. Electric vehicles share the load of the DC mini grid, may store energy dispersedly to boost the DC micro grid's stability and operational performance, support the integration of renewable energy sources, and provide excellent results. The article recommends a three-level CLLC powerful converter for off-board EV battery chargers as a means to provide bidirectional power transfer between electric vehicles and the DC micro grid. The substantial series voltage ranges from 200 to 700 volts, which is achieved by combining the two CLLC components with all three complete bridges and their operational parameters. An analogous circuit variant using the first harmonic circuit. A three-level CLLC resonant's main benefit is that it verifies the efficiency. The minimal transformer RMS existing setting is the main operational choice of the circuit. The system's efficacy is shown by the converter's ability to transform a wide variety of result voltages.

Introduction:

In the last five years, dc micro grids have become more powerful and useful in both academic and business settings. Both its efficiency and its friendliness to renewable

Page | 79

[Index in Cosmos](#)

Apr 2024, Volume 14, ISSUE 2

UGC Approved Journal



energy sources (RES) are excellent. There are no issues with reactive power, power quality, frequency policy, or any other issue when this device is connected to the DC bus bar. There are a few issues with dc mini grids, such as dc electrical Arc detection, dc plugs, and dc breakers, in comparison to AC micro grids.

Among them, electric cars have the same average load on dc micro grids; using them as an ESS would save money, space, and power. Through careful management, we may achieve a system that improves the Dc micro grid's overall efficiency while simultaneously increasing its stability and dependability. The ESS's job is to power the bidirectional DC-DC converter, which may switch between two modes: vehicle-to-grid and grid-to-car. This needs an off-board charger for the electric vehicle.

PROPOSED THREE-LEVEL CLLC RESONANT CONVERTER :-

A. The topology of the three-level CLLC resonant converter :-

Two three-level full bridges and a one-of-a-kind frequency transformer that uses two resonant inductors and capacitors (L_{r1} , L_{r2} and C_{r1} , C_{r2}) make up the bulk of it. The CLLC converter's totally balanced architecture makes it obvious that it can function in two ways. The primary bridge functions as an inverter and the secondary bridge as a rectifier when the converter is in the G2v mode. But the switch flips to G2v mode while the converter is in the V2G mode.

B. How the essential three-level complete bridge functions: -.

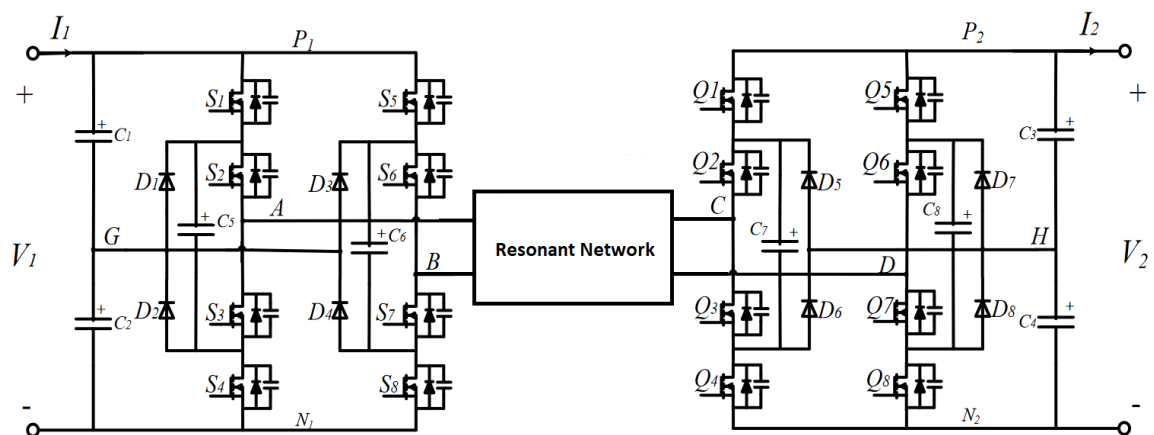
With the primary three-level full bridge, a voltage waveform with a non-zero mean value may be generated. There will be very little change to the Dc component of V_{ab} due to the strong capacitor. Consistently, V_{ab} is the value of the ordinary voltage across capacitor C_{r1} . The three-level leg has four different states it may run in at once. By activating s_1



and s_2 while deactivating s_3 and s_4 , for instance, one may get positive voltage. A three-level main bridge leg's switching states are P, O1, O2, and N. There is no change (i_p) in the voltage of flying capacitor C_5 for states P and N. The C_5 voltage is affected in different ways by the current i_p for the O1 and O2 outcomes. The three-level full bridge may be configured in 16 different ways using only two three-level legs. There are four possible modes of operation for the main three-level full bridge, depending on the changing situation. Modes A, B, C, and D are examples of this.

The secondary three-level full bridge's operational parameters are: -.

Common applications include lowering switching losses and recommending certain operating modes for usage in three-level CLLC powerful converter secondary bridges. When both the web link and fly wheel capacitors are in a constant state DC, their voltages are $0.5 v_2$. Details on three more switching states are available for the second bridge in addition to the four main ones. that is, R0, R1, and L2. The polarity of the current determines the voltage that the bridge produces.





FREQUENCY CHARACTERISTICS OF THREE LEVEL CLLC RESONANT CONVERTER

A. Equivalent circuit

At this point, the resonant converter is located close to the resonant frequency in order to enhance regularity. Consequently, it has four distinct modes of operation. During the first three stages of operation, the entire bridge converter generates a voltage that is square wave (VAB). The frequency of resonance in the container, f_0 , is near the regularity f_s .

The three-degree resonant circuit's equal characteristics will disregard the harmonics, and the power will be transferred by relying on the regularity of the switches. A variable resistor may be added to the circuit to allow for method customization; the resistance value is then utilized to calculate the voltage V_2 and current I_2 of the battery. A collection of inductors and capacitors is used in a powerful network.

Because of this, the CLLC converter is equivalent to a strong L-C collection converter. Both LE and CE, which are strong inductance and capacitance equivalents, can control it. $Max = kx/nky$, $LE = Lr1 + n2Lr2$, $K = V2/V1$.

The key components are derived as per the fourier collection formula.

You may calculate the basic component of i_p using this formula if you follow the theory of power conversion.

It is possible to determine the equivalent resistance R_E by using ohm's law.

Selected Operating Mode for Optimal Performance.

There are sixteen different ways that the powerful CLLC converter may work. The current generation of copper and conductor is symmetrical with respect to the square of the number of R.M.s present in the transformer. So, we may do this by reducing loss,



which allows us to pick the converter's operating parameters with the smallest value of transformers R.M.S. that exist.

The root-mean-square (RMS) of i_{p1} is inversely proportional to k_y , as shown in equation (5). Consequently, when k_y achieves its optimal value, the RMS current of the transformer is at its lowest. The comprehensive algorithm is as follows. This can only be accomplished if the strong frequency is somewhat near to the frequency that is changing. What follows is a picture showing how the G2V working mode choice turned out. Optimal operation was associated with voltage conversion ratio but not with active power P . $E > F > G > H$ is the sequence of functional modes that matters most for reducing the working environment with bigger modes. For both the power instructions, to choose the operating modes. The turns ratio of an isolation transformer is calculated using the notion of turn proportions.

Using the CLLC powerful converter in section 3's mode makes it similar to the LC series powerful circuit. Therefore, to accomplish zero voltage switching (ZCS), the changing frequency has to be adjusted up from a strong regularity. As a critical bridge, the MOSFET can do its job. The block diagram of the converter, which may be operated in the G2V mode, is shown in Figure 10. It is easy to change the functioning parameters of three-degree bridges using v_1 and v_2 , according to the choosing algorithm. When the pulse regularity module is in primary operating mode, it sets the switching frequency and makes the pulse. As described in section c, the second bridge provides information on the converter's extra functional settings, including how it determines the changing settings of the three level legs. When operating in V2G mode, the converter takes charge of I_1 . The existing controller depends on the error to provide switching regularity, namely pulse regularity modulation (PFM), which in turn generates gate pulses for the new bridge based on its switching mode and working mode.

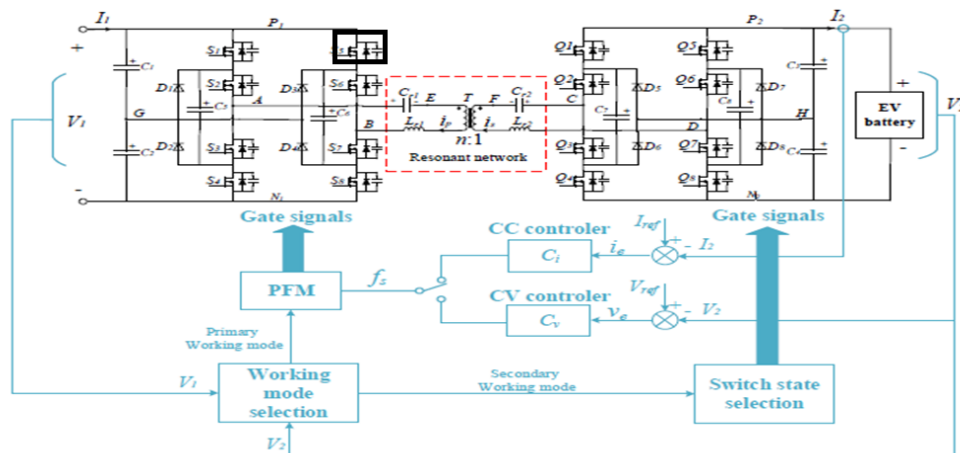
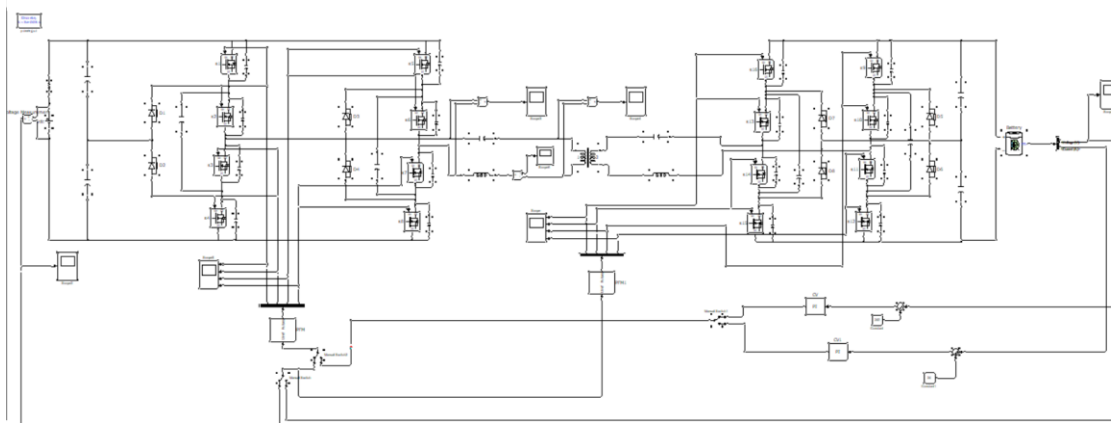


Fig. 10. The control block diagram when the converter operates in G2V mode

PI SIMULINK MODEL :



Simulation Results

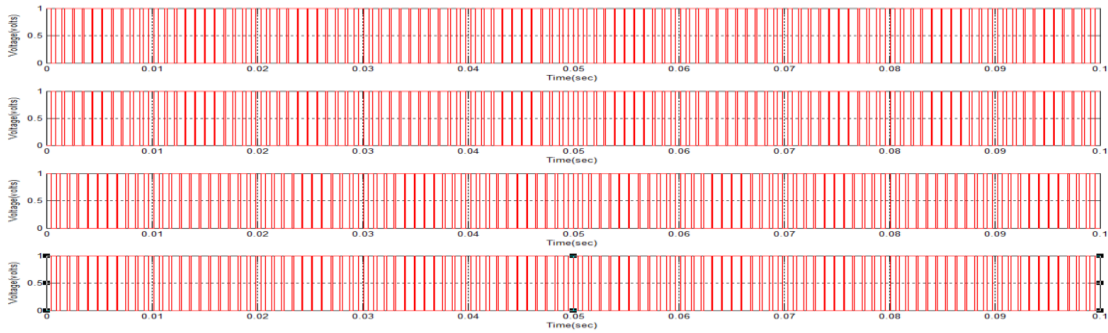
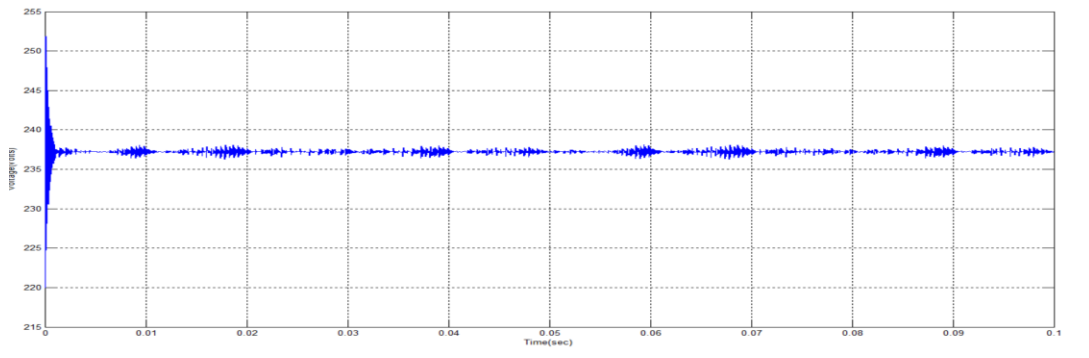


Fig (a): The actual switching frequency for the experiment



Fig(b): Four working modes of the secondary full bridge in the three level CLLC converter

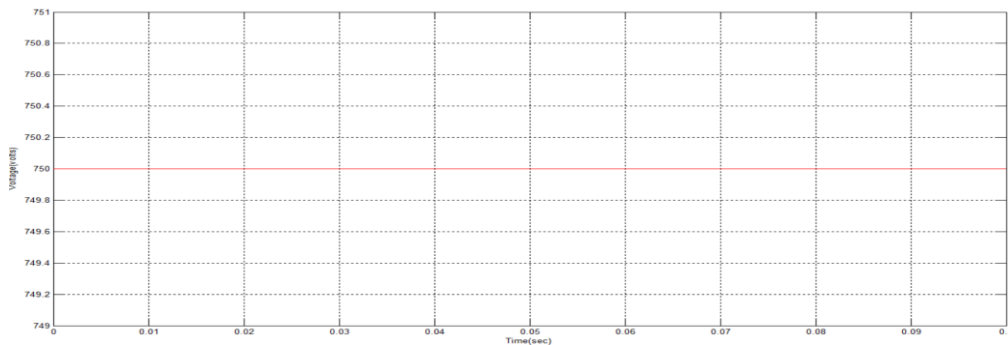
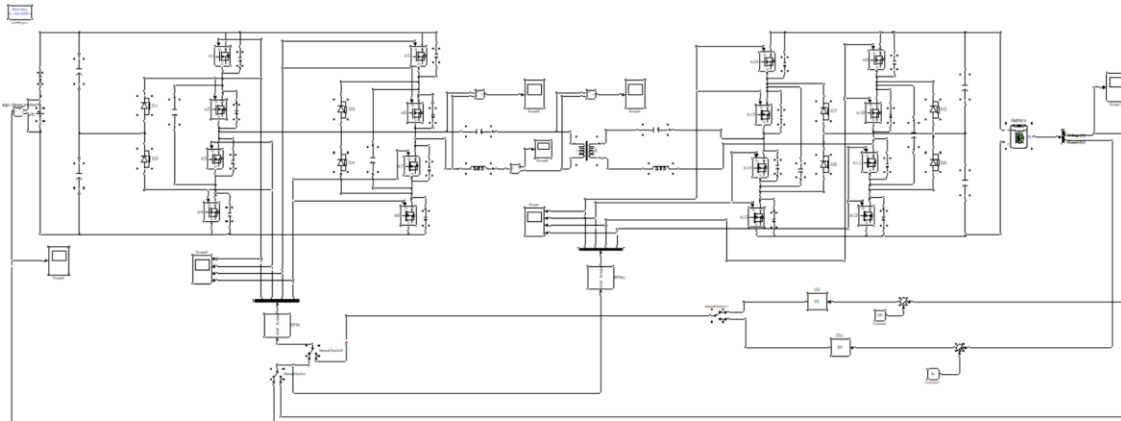


Fig (c): Three level CLLC converter using secondary full bridge



PID SIMULINK MODEL



Simulation Results

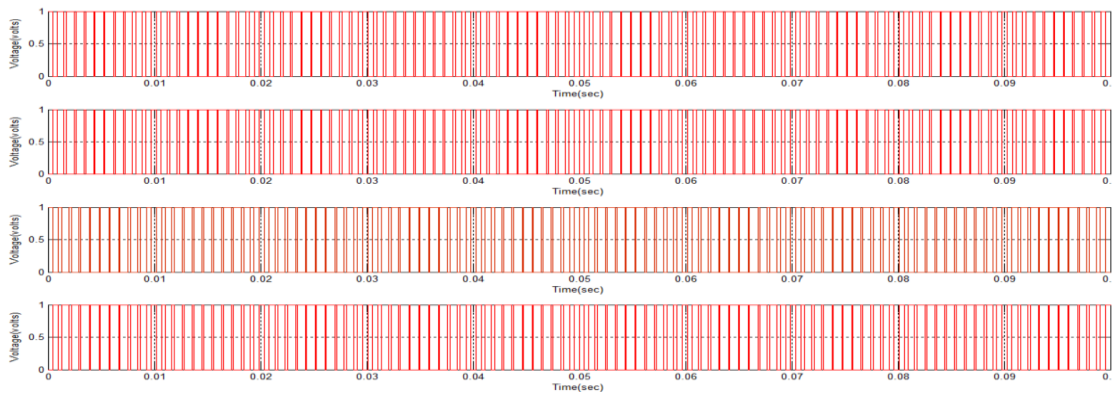


Fig (a): Four working modes of the primary full bridge

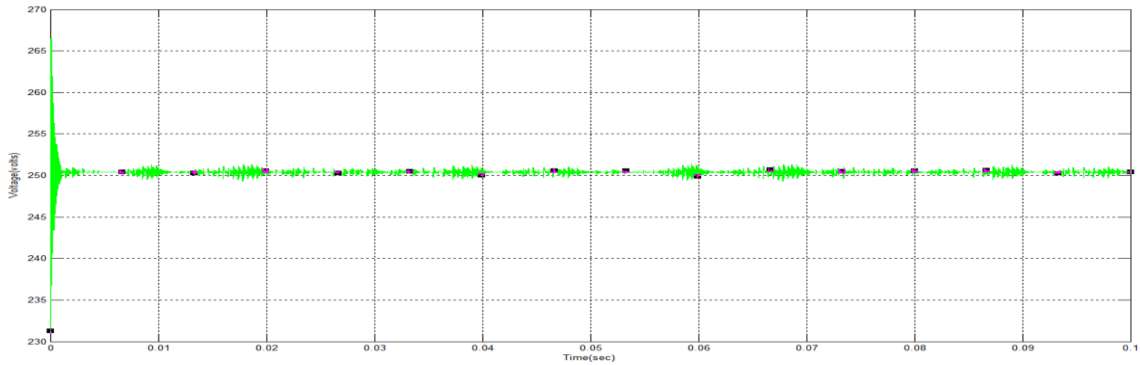


Fig (b): Working mode of full bridge converter

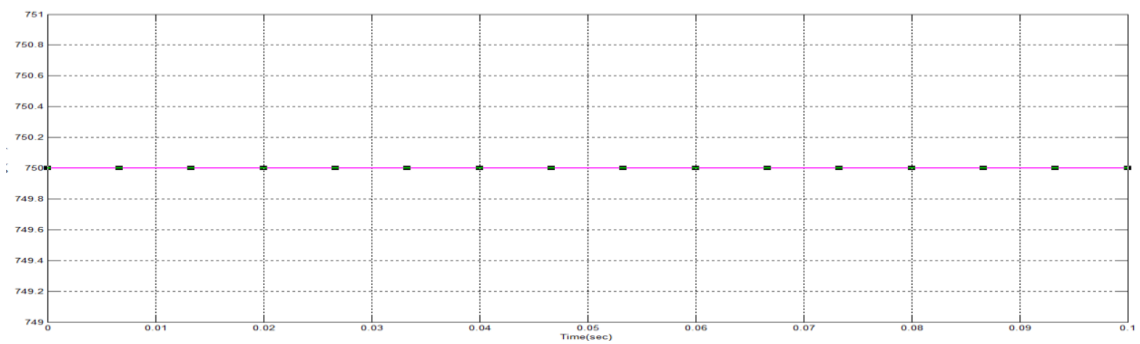


Fig (c): Working mode of primary full bridge at mode D

Conclusion:

For DC micro-grids that use off-board EV battery chargers, this study proposes a three-level CLLC powerful converter. There are four possible modes of operation for the converter's two 3-degree complete bridges. The suggested converter is versatile enough to handle applications with a wide variety of output voltages since it combines the operating modes of the two total bridges. The frequency attributes are investigated using the same circuit as a three-level CLLC strong converter that has been developed with FHA breakthrough. We advise using a calculation based on the existing minimal transformer



RMS to determine the operating settings. The proposed converter was tested using a 3.5 W prototype device. The results of the simulations show that the converter can remain stable across a wide range of output voltages, and the efficiency of the suggested converter changes somewhat beyond that range. In addition, by choosing different switching states in different switching cycles, the three-level CLLC powerful converter's flying capacitor voltages are now stabilized.

References

- [1] M. Granovskii, I. Dincer, and M. A. Rosen, "Economic and environmental comparison of conventional, hybrid, electric and hydrogen fuel cell vehicles," *J. Power Sources*, vol. 159, no. 2, pp. 1186–1193, 2006.
- [2] S. B. Peterson, J. Whitacre, and J. Apt, "The economics of using plug-in hybrid electric vehicle battery packs for grid storage," *J. Power Sources*, vol. 195, no. 8, pp. 2377–2384, 2010.
- [3] Y. Zhou, M. Wang, H. Hao, L. Johnson, and H. Wang, "Plug-in electric vehicle market penetration and incentives: A global review," *Mitigation Adaptation Strategies Global Change*, vol. 20, no. 5, pp. 777–795, 2015.
- [4] B. Nykvist and M. Nilsson, "Rapidly falling costs of battery packs for electric vehicles," *Nature Climate Change*, vol. 5, no. 4, pp. 329–332, 2015.
- [5] W. Zhang and C. C. Mi, "Compensation topologies of high-power wireless power transfer systems," *IEEE Trans. Veh. Technol.*, vol. 65, no. 6, pp. 4768–4778, Jun. 2016.
- [6] K. Mude and K. Aditya, "Comprehensive review and analysis of two-element resonant compensation topologies for wireless inductive power transfer systems," *Chin. J. Elect. Eng.*, vol. 5, no. 2, pp. 14–31, 2019.
- [7] Y. Jiang, L. Wang, Y. Wang, J. Liu, X. Li, and G. Ning, "Analysis, design, and implementation of accurate ZVS angle control for EV battery charging in wireless



high-power transfer,” *IEEE Trans. Ind. Electron.*, vol. 66, no. 5, pp. 4075–4085, May 2019.

[8] Y. Jiang, L.Wang, Y.Wang, J. Liu, M.Wu, and G. Ning, “Analysis, design, and implementation of WPT system for EV’s battery charging based on optimal operation frequency range,” *IEEE Trans. Power Electron.*, vol. 34, no. 7, pp. 6890–6905, Jul. 2019.

[9] D. H. Tran, V. B. Vu, and W. Choi, “Design of a high-efficiency wireless power transfer system with intermediate coils for the on-board chargers of electric vehicles,” *IEEE Trans. Power Electron.*, vol. 33, no. 1, pp. 175–187, Jan. 2018.

[10] S. Moon and G.-W. Moon, “Wireless power transfer system with an asymmetric four-coil resonator for electric vehicle battery chargers,” *IEEE Trans. Power Electron.*, vol. 31, no. 10, pp. 6844–6854, Oct. 2016.

[11] O. C. Onar, M. Chinthavali, S. L. Campbell, L. E. Seiber, and C. P. White, “Vehicular integration of wireless power transfer systems and hardware interoperability case studies,” *IEEE Trans. Ind. Appl.*, vol. 55, no. 5, pp. 5223–5234, Sep./Oct. 2019.

[12] S. Li, W. Li, J. Deng, T. D. Nguyen, and C. C. Mi, “A double-sided LCC compensation network and its tuning method for wireless power transfer,” *IEEE Trans. Veh. Technol.*, vol. 64, no. 6, pp. 2261–2273, Jun. 2015.

[13] C. Liu, S. Ge, Y. Guo, H. Li, and G. Cai, “Double-LCL resonant compensation network for electric vehicles wireless power transfer: Experimental study and analysis,” *IET Power Electron.*, vol. 9, no. 11, pp. 2262–2270, 2016.

[14] C. Xiao, D. Cheng, and K. Wei, “An LCC-C compensated wireless charging system for implantable cardiac pacemakers: Theory, experiment, and safety evaluation,” *IEEE Trans. Power Electron.*, vol. 33, no. 6, pp. 4894–4905, Jun. 2018.

[15] Y. Chen, H. Zhang, S.-J. Park, and D.-H. Kim, “A switching hybrid LCC-S compensation topology for constant current/voltage EV wireless charging,” *IEEE Access*, vol. 7, pp. 133924–133935, 2019.



- [16] Y. Zhang, Z. Yan, T. Kan, Y. Liu, and C. C. Mi, “Modelling and analysis of the distortion of strongly-coupled wireless power transfer systems with SS and LCC–LCC compensations,” *IET Power Electron.*, vol. 12, no. 6, pp. 1321–1328, 2019.
- [17] W. Li, H. Zhao, J. Deng, S. Li, and C. C. Mi, “Comparison study on SS and double-sided LCC compensation topologies for EV/PHEV wireless chargers,” *IEEE Trans. Veh. Technol.*, vol. 65, no. 6, pp. 4429–4439, Jun. 2016.
- [18] G. N. B. Yadav and N. L. Narasamma, “An active soft switched phaseshifted full-bridge dc–dc converter: Analysis, modeling, design, and implementation,” *IEEE Trans. Power Electron.*, vol. 29, no. 9, pp. 4538–4550, Sep. 2014.
- [19] M. Pahlevaninezhad, P. Das, J. Drobnik, P. K. Jain, and A. Bakhshai, “A novel ZVZCS full-bridge dc/dc converter used for electric vehicles,” *IEEE Trans. Power Electron.*, vol. 27, no. 6, pp. 2752–2769, Jun. 2012.
- [20] V. R. K. Kanamarlapudi, B. Wang, P. L. So, and Z. Wang, “Analysis, design, and implementation of an APWM ZVZCS full-bridge dc–dc converter for battery charging in electric vehicles,” *IEEE Trans. Power Electron.*, vol. 32, no. 8, pp. 6145–6160, Aug. 2017.
- [21] J. K. Nama, M. Srivastava, and A. K. Verma, “Modified inductive power transfer topology for electrical vehicle battery charging using auxiliary network to achieve zero-voltage switching for full load variations,” *IET Power Electron.*, vol. 12, no. 10, pp. 2513–2522, 2019.